Electronic Supplementary Information (ESI)

(12 pages)

Reversible Solid-State Reaction between 18-Crown[6] and M[H_2PO_4] (M = K, Rb, Cs) and an Investigation of the Decomplexation Process

Dario Braga, Marco Polito, Elena Dichiarante, Katia Rubini, and Fabrizia Grepioni

Packing patterns, DSC and TGA measurements, and X-ray powder patterns for the complexes 18-Crown[6]·K[H_2PO_4]·2H_2O (**1**), 18-Crown[6]·Rb[H_2PO_4]·2H_2O (**2**) and 18-Crown[6]·Cs[H_2PO_4] ·1.5H_2O (**3**).

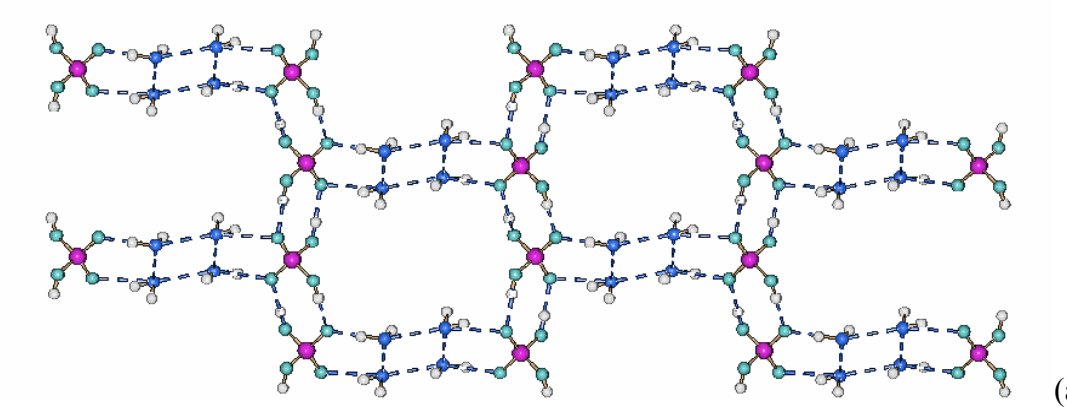

(a)

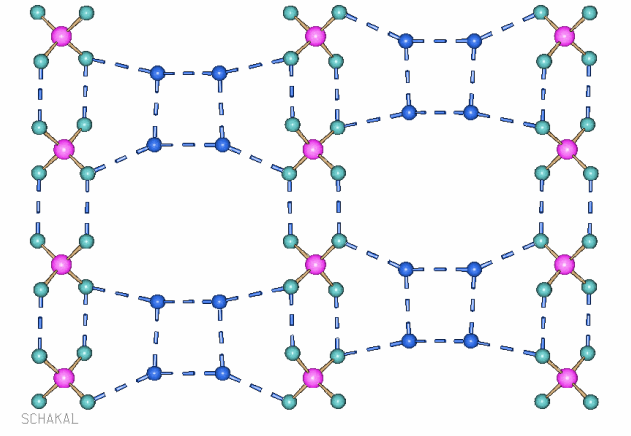

(b)

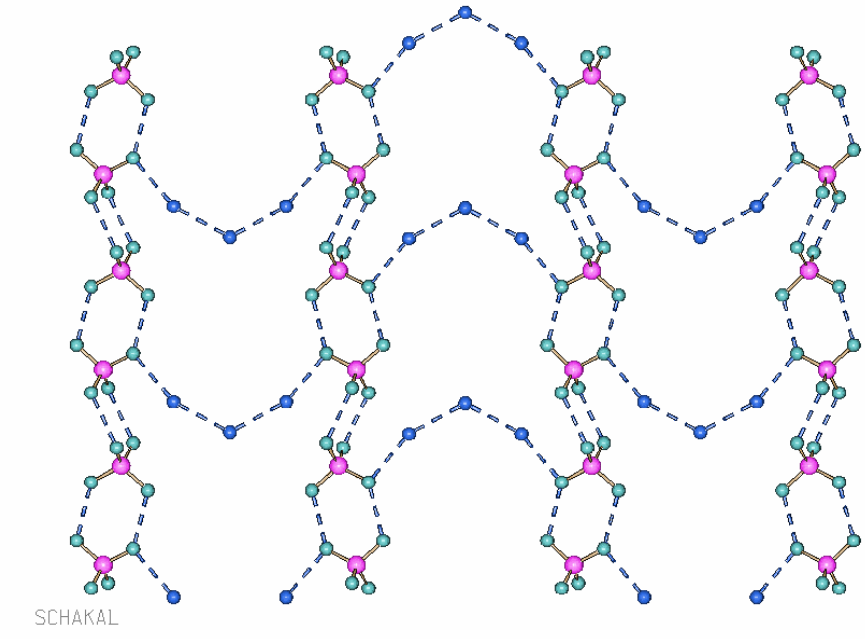

(c)

Figure ESI-1. Dihydrogen phosphate anions and water molecules form two-dimensional networks in the crystals of the (a) potassium, (b) rubidium and (c) caesium complexes; the water molecules act as bridges between the dihydrogen phosphate chains (H_{OH} atoms not observed in the rubidium and caesium complexes).

18-Crown[6]·K[H_2PO_4]·2H_2O (**1**)

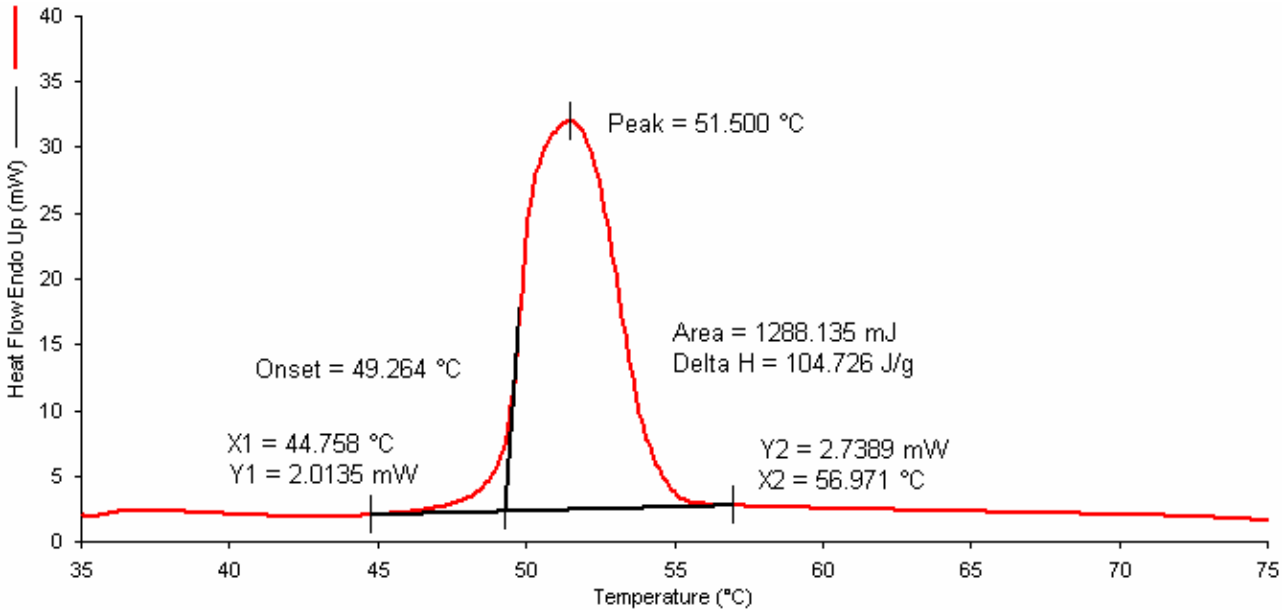

Figure ESI-2. DSC trace (heating cycle) for compound **1**.

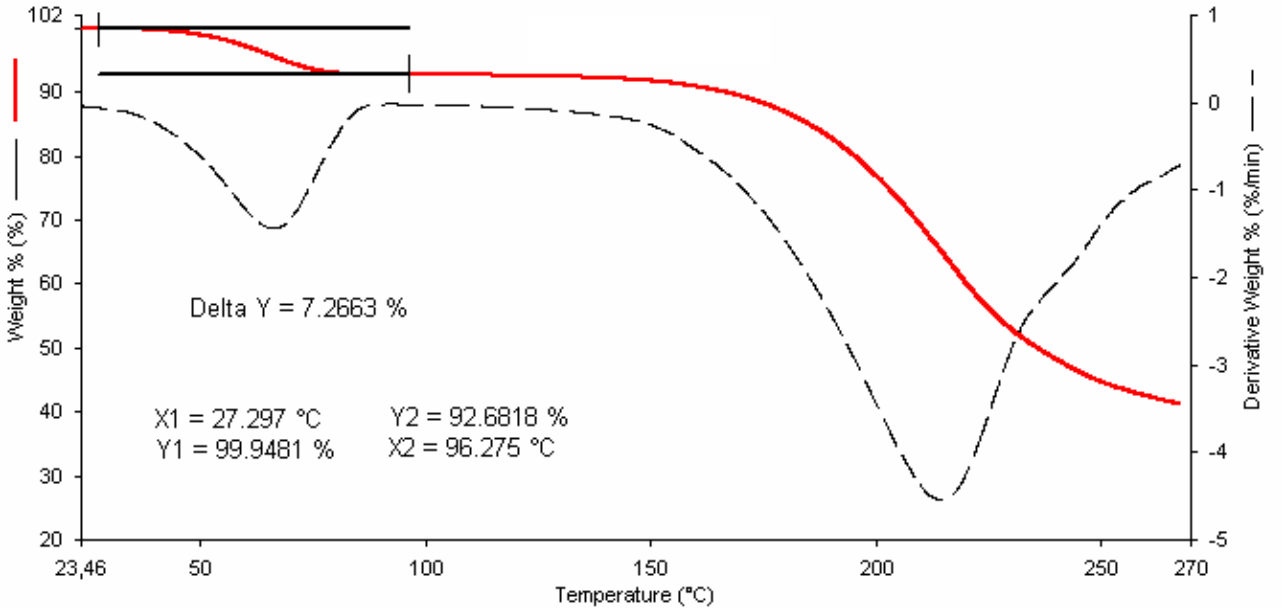

Figure ESI-3. TGA measurement for compound **1**.

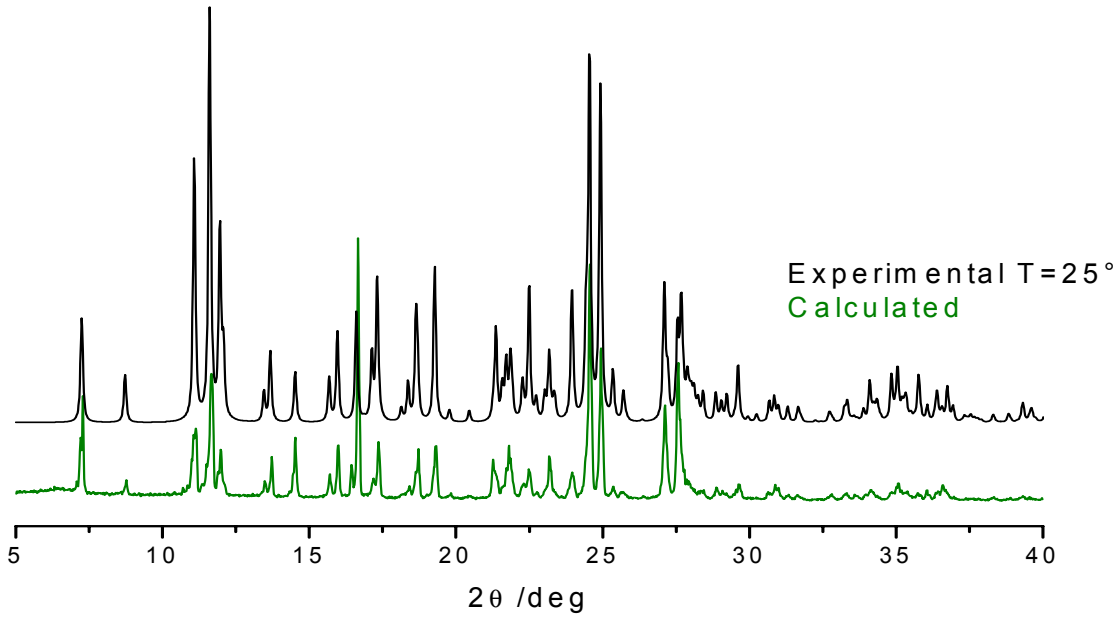

Figure ESI-4. Comparison between the experimental (top) and calculated (bottom)X-ray powder diffraction patterns for compound **1**.

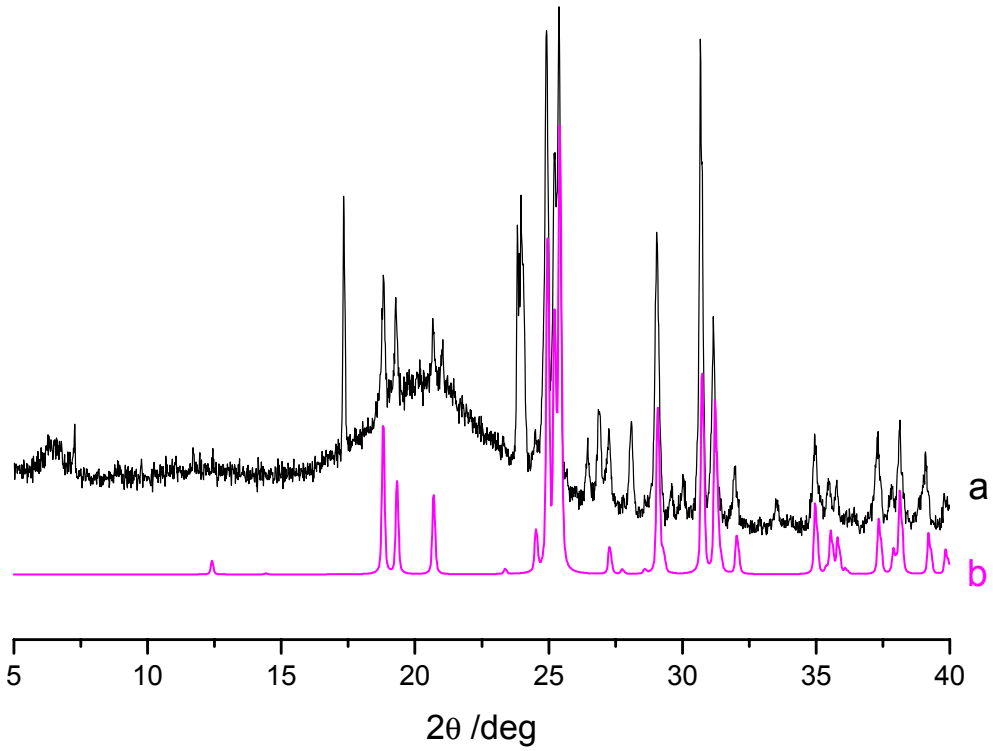

Figure ESI-5. Comparison between (a) the experimental X-ray powder diffraction pattern of complex **1** at 70°C and (b) the calculated pattern of $K[H_2PO_4]$.

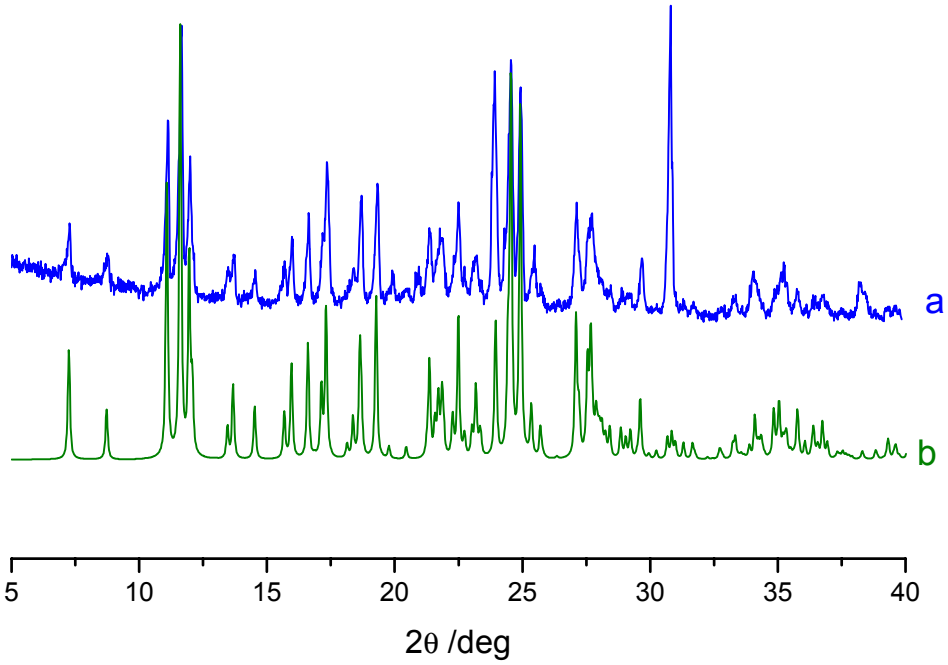

Figure ESI-6. Comparison between the diffractogram of **1** (ground material) after treatment at 70°C (a) and the calculated pattern for the starting material **1** (b).

18-Crown[6]·$Rb[H_2PO_4]$·$2H_2O$ (**2**)

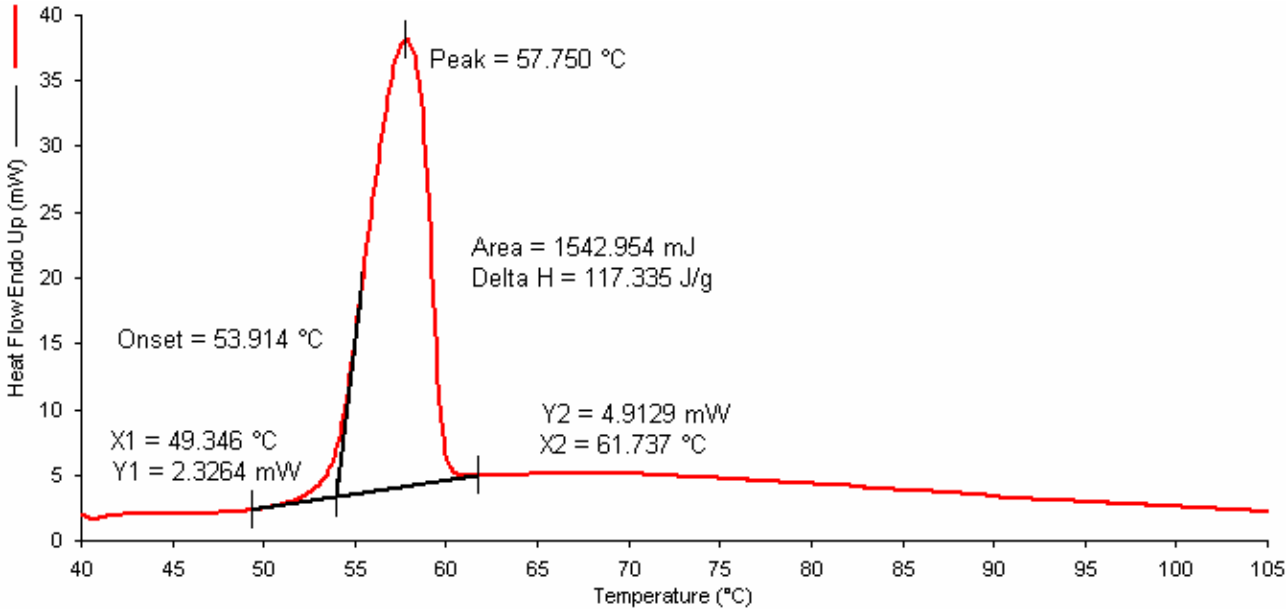

Figure ESI-7. DSC trace (heating cycle) for compound **2**.

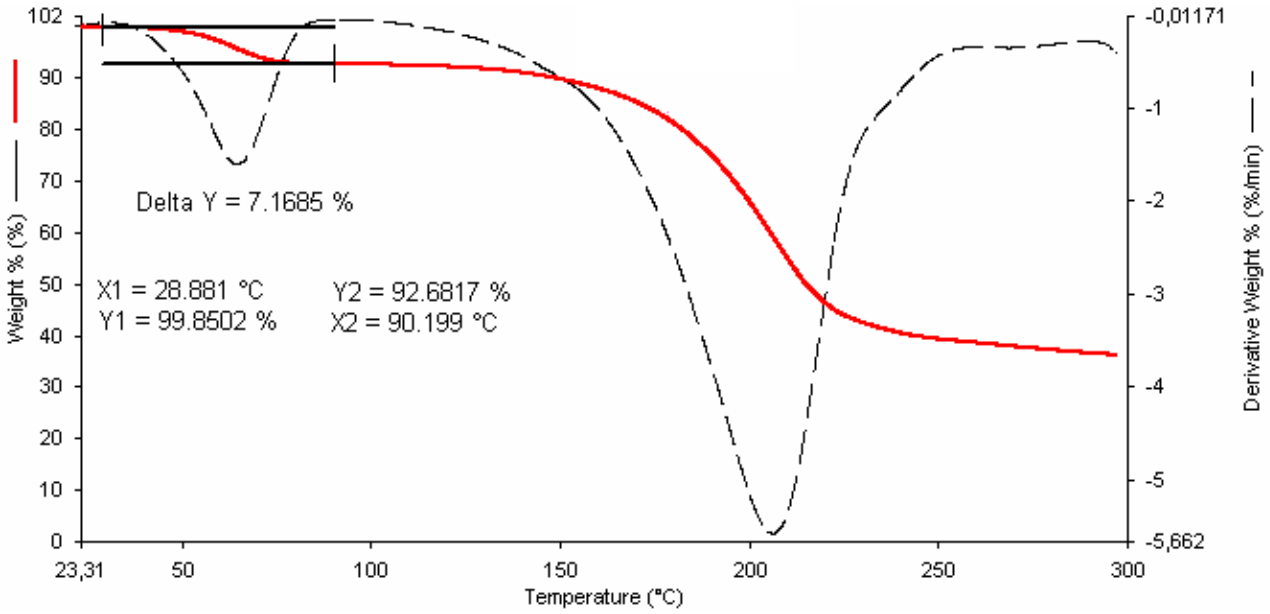

Figure ESI-8. TGA trace for compound **2**.

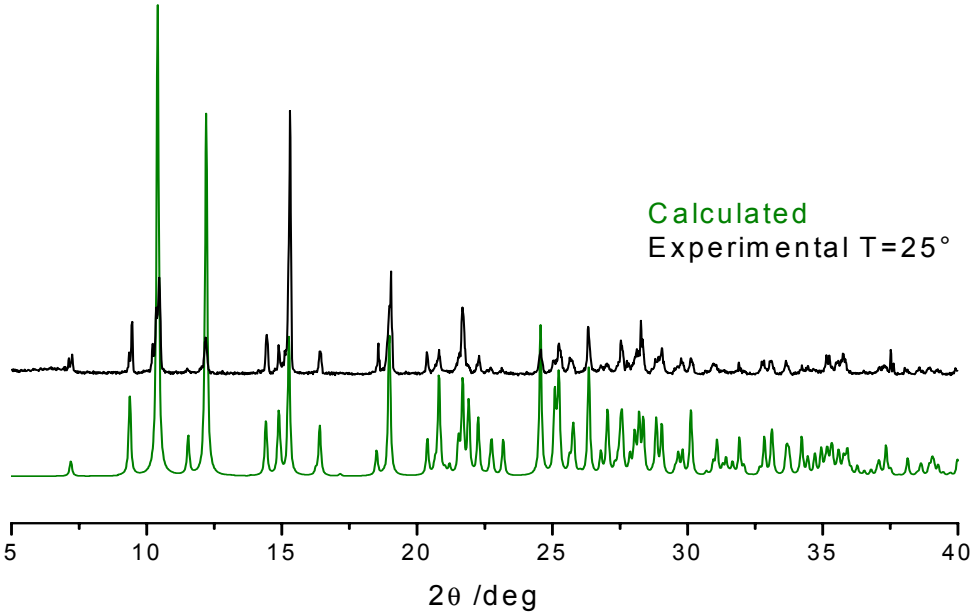

Figure ESI-9. Comparison between experimental (top) and calculated (bottom) X-ray powder diffraction patterns for compound **2**.

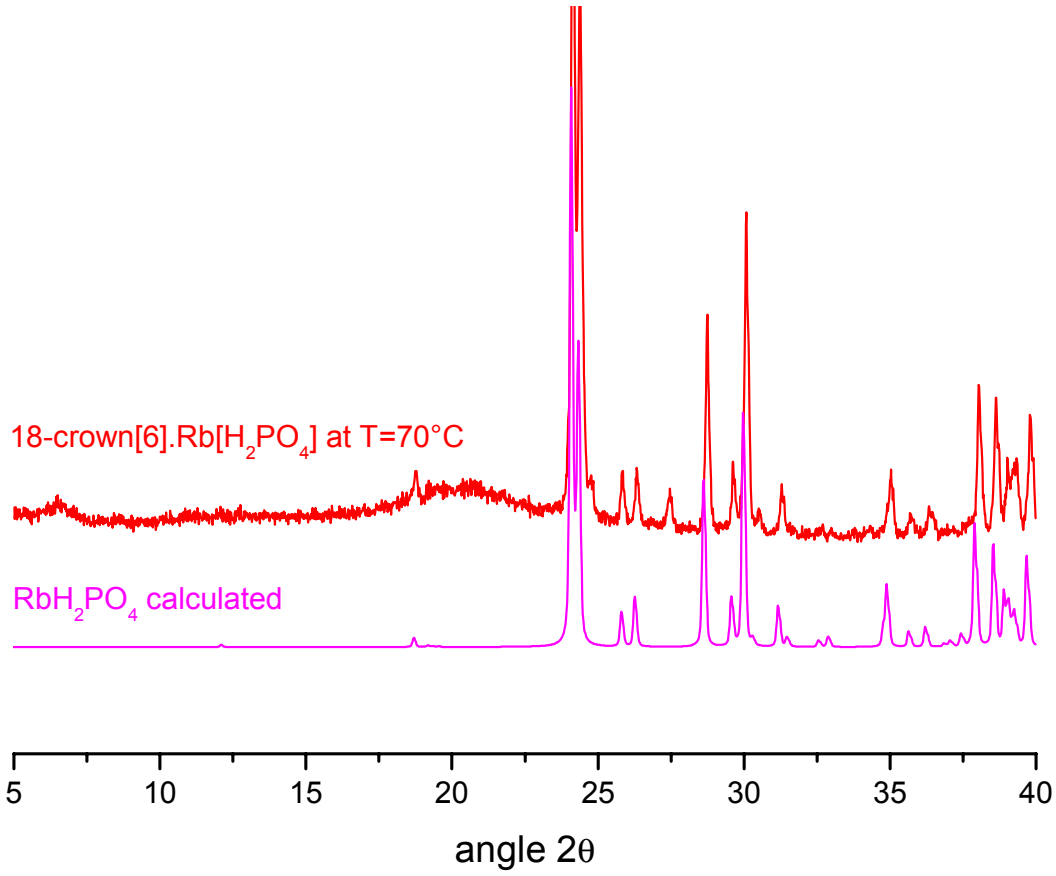

Figure ESI-10. Comparison between (top) the experimental X-ray powder diffraction pattern of **2** at 70°C and (bottom) the calculated pattern of $Rb[H_2PO_4]$.

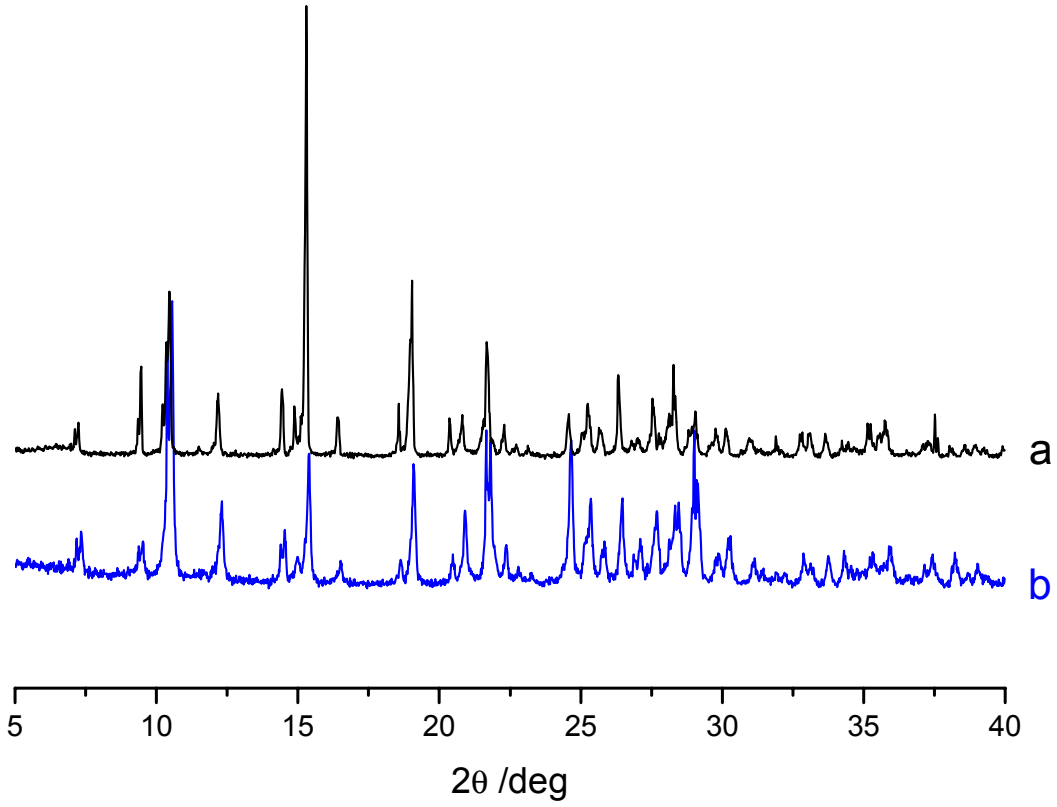

Figure ESI-11. Comparison between the diffractogram of the starting material **2** (a) and the diffractogram of the ground material after treatment at 70°C (b).

18-Crown[6]·Cs[H_2PO_4] ·1.5H_2O (**3**)

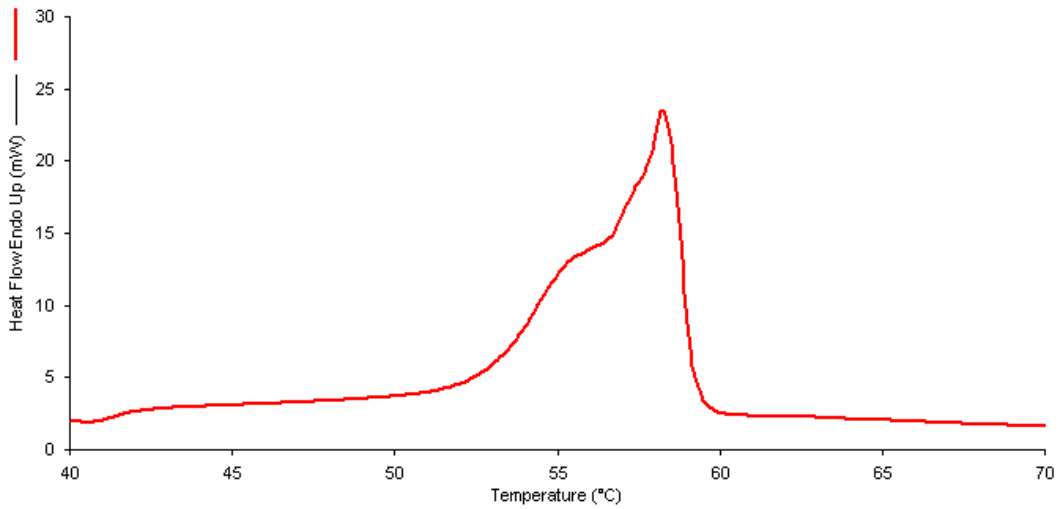

Figure ESI-12. The DSC trace of a sample of **3** (heating cycle). Note the single, though asymmetric, endothermic peak (onset at 56.4°C, ΔH = 79.2 J g^{-1}) due to loss of water, extrusion of crown ether from the crystalline complex and reconstruction of crystalline Cs[H_2PO_4].

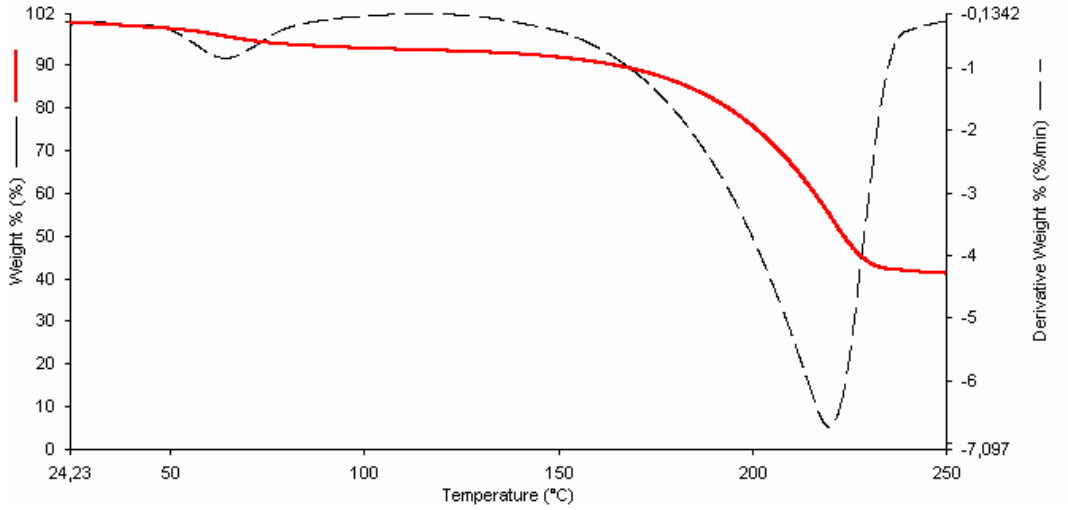

Figure ESI-13. The TGA trace of **3** shows a weight loss of ca. 5.2% in the interval 40°-100°C, in agreement with a loss of 1.5 moles of water. Further heating shows evaporation of the crown ether at ca. 200 °C

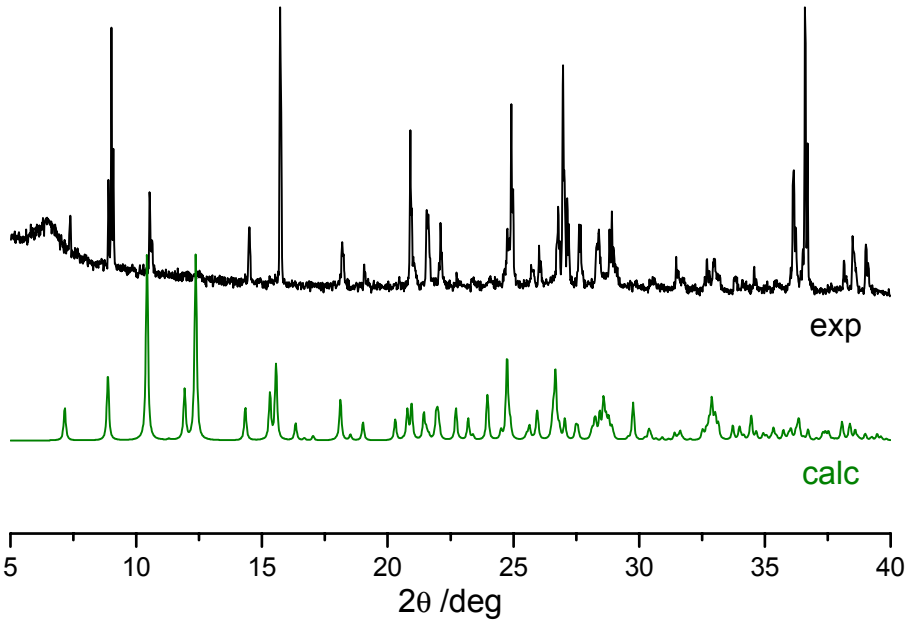

Figure ESI-14. Comparison between the diffraction pattern measured on a polycrystalline sample of **3** and that calculated on the basis of the single crystal structure.

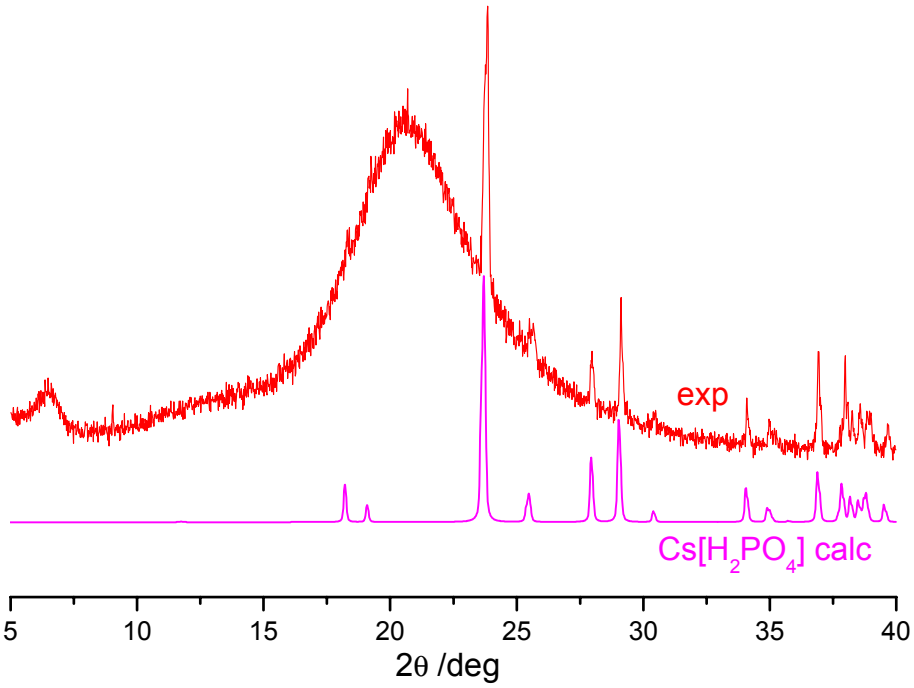

Figure ESI-15. Heating the complex **3** to 60°C leads to a mixture of an amorphous phase superimposed to a crystalline phase, which has been identified as anhydrous $Cs[H_2PO_4]$.

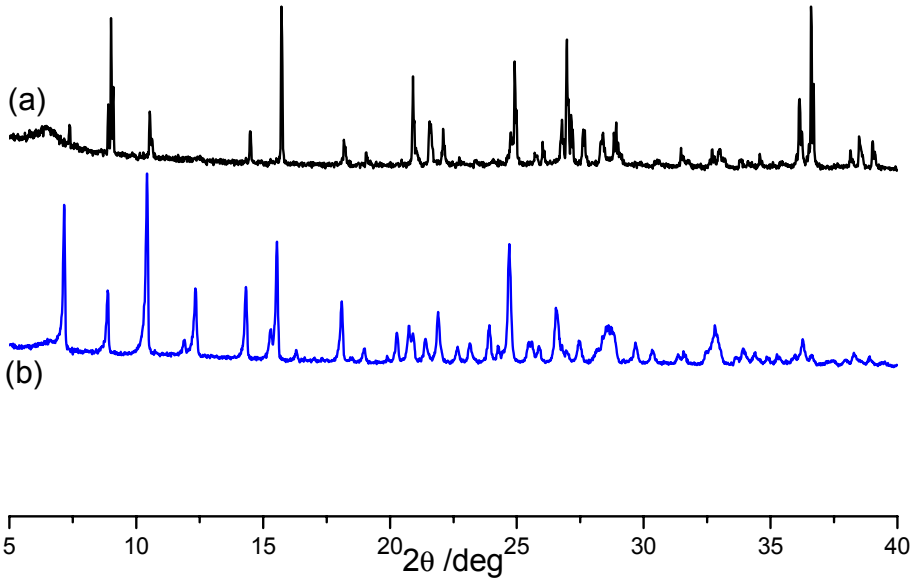

Figure ESI-16. Comparison between the diffractogram of the starting material **3** (a) and the diffractogram of the ground material after treatment at 60°C (b).

N.B.: Thermal treatment on compounds 1, 2 and 3 , in the variable temperature X-ray powder diffraction experiments, was performed at the minimum temperature required for the decomplexation process to occur, i.e. at 70°C for 1 and 2, and at 60°C for 3.
